JOURNAL OF SPACECRAFT AND ROCKETS
Vol. 37, No. 5, September–October 2000

Charging of Composites in the Space Environment

Steven A. Czepiela,* Hugh McManus,† and Daniel Hastings‡
Massachusetts Institute of Technology, Cambridge, Massachusetts 02139

The space environment includes high-energy charged particles, which deposit in the composite materials of satellites. The deposited particles create an electric field, which may grow until an electrostatic discharge occurs. A one-dimensional finite difference model has been developed, which calculates the electric field in space and time as a function of the environment, material properties, and boundary conditions. Using the electron and proton flux for a 7000-km-altitude orbit and the material data for a typical organic polymer, the calculated steady-state electric field is approximately 4400 V/m with a steady-state development time of 1.3 s. This is several orders of magnitude lower than the dielectric strength of the material, 15 MV/m. Based on sensitivity studies done by varying particle fluxes and material properties several orders of magnitude around typical values, it was concluded that typical flux levels do not cause significant deep dielectric charging in typical composite materials. However, discharges can occur during substorms when particle flux levels can rise by several orders of magnitude.

Nomenclature

$\dot{D}$	=	dose rate, rad/s
E	=	electric field, V/m
h_{SL}	=	thickness of epoxy surface layer, m
J	=	current density, A/m^2
k_R	=	coefficient of radiation induced conductivity, s/Ω-m-rad
t	=	time, s
V	=	voltage, V
x	=	depth into material, m
Δ	=	material parameter associated with radiation induced conductivity
ε_0	=	permittivity of free space, C^2/N-m^2
κ	=	dielectric constant
ρ	=	charge density, #/m^3
ρ_m	=	mass density, kg/m^3
$\dot{\rho}_{in}$	=	incoming charge density rate, #/m^3-s
σ	=	dark conductivity, 1/Ω-m
σ_R	=	radiation induced conductivity, 1/Ω-m

Introduction

THE charging of spacecraft, and its role in spacecraft anomalies as a result of electrostatic discharges, is well known.[1] Charging is caused by energetic particles in the space environment. The main sources of these particles are the Van Allen radiation belts, solar flares and substorms, and galactic cosmic rays. There are two types of charging, surface charging and internal charging, also known as deep dielectric charging. Most of the work done up until now has been on surface charging. It is caused by low-energy electrons (30–50 keV), which do not penetrate the surface of the material. This charging can grow large enough to cause an electrostatic discharge, which can lead to spacecraft anomalies. During the 1970s and 1980s, protection techniques were developed that have basically taken care of the surface charging problem.[2] Because anomalies continue to occur on spacecraft, investigation of deep dielectric charging is required.

Deep dielectric charging occurs when high-energy electrons or ions penetrate the surface of, and deposit charge within, a dielectric material. If the deposition of incoming charged particles is greater than the charge leakage through the material, a large potential difference can build up in the material and lead to a discharge. Several spacecraft failures have been associated with electrostatic discharges resulting from deep dielectric charging, including the $300 million Telesat Canada communications satellites ANIK E1 and E2 and the ESA spacecraft Olympus. Other spacecraft have experienced switchings or anomalies as a result of electrostatic discharges resulting from deep dielectric charging, including Intelsat K, ECS-2 and ECS-4, and the Combined Release and Radiation Effects Spacecraft.[3] Although some spacecraft have been affected by deep dielectric charging, other spacecraft of similar design and in operation at the same time have not been affected.

Some early modeling of deep dielectric charging was done by Berkley[4] and Frederickson and Woolf.[5] Berkley included in his model the effects of nonuniform time-varying radiation induced conductivity and charges obtained from a single-scattering Monte Carlo calculation of the nonrelativistic electron-beam/dielectric interaction. Frederickson and Woolf[5] basically used the same model but improved the calculations to include the dose effects of secondary x rays and bremsstrahlung and the effect of electric fields on the primary electron transport. Both of these models work well, but do not simulate the space environment, as they work only for an electron beam of monoenergetic electrons. Recently Soubeyran et al. (Soubeyran, A., Estienne, J. P., Borde, J., and Drolshagen, G., "Numerical Simulation of Bulk Charging," unpublished paper, 1997, pp. 1–13) developed European Space Agency Deep Dielectric Charging, a numerical tool to analyze deep dielectric charging in the space environment. The model uses Monte Carlo particle transport codes to track the path followed by the electrons and protons, following which Ampere's equation with Ohm's law are solved for the electric field in the material.

Most previous work on deep dielectric charging has dealt with the charging of spacecraft components such as wire insulation and printed circuit boards, where electrostatic discharges can lead to anomalies in spacecraft operation. However, with the increasing use of composite materials, which can be dielectrics, deep dielectric charging is an increasing problem in the structure of spacecraft.

In this paper a simple one-dimensional model of deep dielectic charging in composite materials is developed. It is used to analyze the behavior of typical composite materials under typical space conditions. Parametric analyses around a baseline case show that, even given uncertainties in flux levels and material properties, typical conditions do not create problematic levels of charging. However, analysis of conditions typical of a severe substorm show that levels of charging can occur that create electric fields strengths close to the breakdown strength of the material.

Theory

Composites

Composites are starting to replace metals on the structure of spacecraft, caused primarily by their higher stiffness-to-weight

Presented as Paper 97-0629 at the AIAA 35th Aerospace Sciences Meeting, Reno, NV, 6–9 January 1997; received 18 March 1998; revision received 25 April 2000; accepted for publication 25 April 2000.

*Research Assistant, Department of Aeronautics and Astronautics. Student Member AIAA.
†Associate Professor, Department of Aeronautics and Astronautics. Associate Fellow AIAA.
‡Professor, Department of Aeronautics and Astronautics. Fellow AIAA.

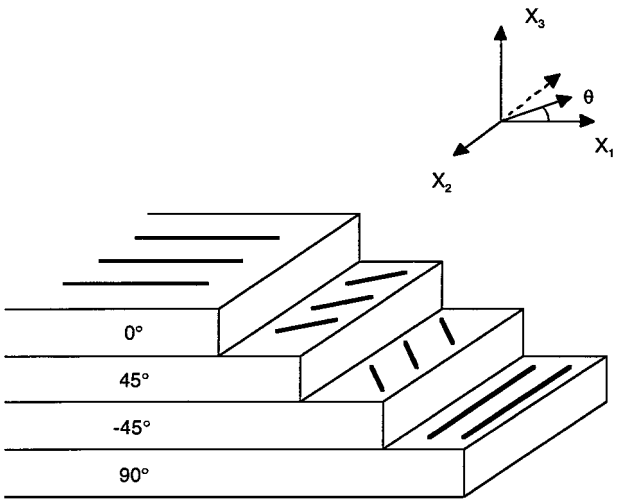

Fig. 1 Typical composite laminate in the geometric coordinate system.

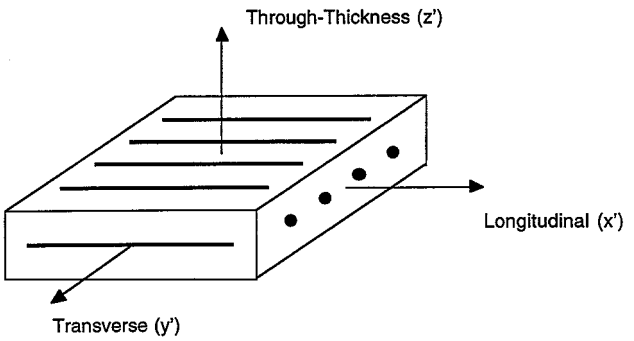

Fig. 2 Typical ply in the ply coordinate system.

ratios. Composites are made up of multiple layers or plies, which are stacked at various angles to get the desired material properties. These plies are in turn made up of fibers and a matrix material that surrounds the fiber. The dominant fibers used are carbon (sometimes referred to as graphite), glass, and Kevlar, and the dominant matrix materials are epoxies, cyanates, and poly-ether-ether-ketones.

By varying the angles of the plies and the stacking sequence of the plies (Fig. 1), one can tailor the properties of the laminate or composite structure. The ply angles affect the material properties because the plies are anisotropic. The material properties in the longitudinal direction can be very different from the properties in the transverse and through-thickness directions (Fig. 2). The ply angle is defined as the angle between the geometric coordinate system and the ply coordinate system. The geometric coordinate system is arbitrarily assigned to a structural direction, for example, the length of a solar panel array, and the ply coordinate system is aligned with the fiber direction, as shown in Figs. 1 and 2. Therefore a 0-deg ply will have its longitudinal properties aligned with the principal direction of the structure, whereas a 90-deg ply will have its transverse properties aligned with the principal direction of the structure. The laminate properties are based on the ply properties and the ply angles and can be calculated using classical laminated plate theory.

In modeling composites the bulk properties of the composite ply are generally used instead of the individual properties of the fibers and matrix. This is an acceptable simplification for a first-order solution of the problem because the thickness of the material is much greater than the diameter of the fibers. To determine the ply properties, one has to combine the fiber properties with the matrix properties. The ply properties depend on the volume fraction of fiber used in the composite material. There are many models that are used to determine the ply properties, all of which have modeling limitations. Typically the simplest models are for the longitudinal direction. These models are generally independent of the details of the fiber and matrix geometry. They are reviewed in Ref. 6.

However, the details of the fiber and matrix arrangement can matter, especially in cases where the properties of the fiber and matrix differ radically. This is the case with electrical properties, where the details of the geometry can be important, as in the case of a low-resistance chain of fibers (referred to as a percolation path) or an insulating epoxy-rich surface layer on the composite. These details will be examined on a case-by-case basis.

Charging

The basic problem is that high-energy particles from the space environment penetrate the surface of the composite material and lose energy until they stop somewhere within the material. These stopped particles induce an electric field within the material. This electric field causes the particles to move, causing a current in the material. This current in turn influences the electric field. The electric field continues to grow until equilibrium is reached between the flux of incoming particles and the particle flux leaving because of the current. Another possibility is that the electric field exceeds the dielectric strength of the material before equilibrium is reached, and a breakdown and subsequent electrostatic discharge occurs. Here, a model of this process is described. A FORTRAN code based on this model, which calculates the electric field and charge density until one of the two just mentioned possibilities occur, was written. Magnetic field effects are assumed to be negligible because of the low current density ($\lesssim$10 nA/cm^2) and low velocity of charge carriers in dielectrics ($\lesssim 10^5$ m/s $\ll$ c) (Ref. 7).

The charged particle environment is acquired from the Environmental Workbench (EWB) software.[8] The program runs the electron and proton codes AE8 and AP8 and gives empirical flux data at different energy levels for different altitudes, inclinations, and solar cycle conditions. The particle penetration depth is calculated using empirical information on the stopping power in silicon.[9] The stopping power is given as the linear energy transfer (LET) vs energy. The stopping power in silicon can be used, even though the materials used here are composites, because the LET scales with density. Using the particle flux vs energy distribution from the EWB and the LET curve, the particle flux vs depth of penetration in the material can be calculated. EWB produces a distribution of particles as a function of energy. The LET curve provides the depth a particle penetrates into a material as a function of energy. These two sets of data are combined graphically (or numerically) to produce a distribution of deposited charged particles as a function of depth into the material. The difference between the proton deposition rate and the electron deposition rate then gives the net incoming charge rate as a function of depth.

This is a simpler approach than that used by Soubeyran et al. (unpublished paper), who used a Monte Carlo deposition model. However, a simpler model is acceptable for our work because the model is primarily being used to find order-of-magnitude estimates of the problem and to give direction to the experimental portion of the research. The current approach has the advantages of coupling to an environment model (EWB) and very rapid calculation.

The electric field can be calculated using Gauss's law in differential form[10]:

$$\nabla \cdot \bar{E} = (1/\kappa\varepsilon_0)\rho \tag{1}$$

The charge density includes both the incoming charge density from the space environment and the charge density already in the material. Rewriting Eq. (1) for the one-dimensional case,

$$E = \frac{1}{\kappa\varepsilon_0}\int \rho \, dx \tag{2}$$

The voltage V is calculated directly from the field:

$$V = -\int E \, dx \tag{3}$$

Equations (2) and (3) are solved numerically using the trapezoid rule. Two boundary conditions are required. Either the voltage on both the front and back surface, or any combination of one surface voltage and one surface field, must be specified.

Once the electric field is calculated, the charge density in the material can be calculated with the continuity equation[10]:

$$\nabla \cdot \bar{J} = -\frac{\partial \rho}{\partial t} + \dot{\rho}_{\text{in}} \tag{4}$$

Rewriting Eq. (4) for the one-dimensional case and substituting σE for J,

$$\frac{\partial \rho}{\partial t} = \dot{\rho}_{\text{in}} - \frac{\partial \sigma E}{\partial x} \tag{5}$$

This equation is solved numerically with a central difference in space, explicit in time finite difference routine.

When materials are exposed to radiation, it is known that conductivity of the material increases.[11] This radiation-induced conductivity σ_R is simply added to the dark conductivity of the material. It can be quantitatively related to the dose rate $\dot{D}$ by two material dependent parameters (k_R and Δ):

$$\sigma_R = k_R \dot{D}^{\Delta} \tag{6}$$

Both k_R and Δ have been empirically determined, and Δ is usually between 0.5 and 1.0.

Code

The composite deep dielectric charging analyzer (CoDDCA) can determine the electric field and charge density as a function of depth into a composite material in a specified orbital environment, and thus predict if an electrostatic discharge will occur. CoDDCA can be run for any orbit by specifying the orbit parameters (the apogee, perigee, inclination, and solar cycle condition) in EWB. The material is also user specified. The material is characterized electrically by its conductivity, dielectric constant, and dielectric strength, and structurally by the material thickness and boundary conditions. There is also an option to include radiation-induced conductivity. The code is available on request from the authors.

Results

Base Case

In this section results are presented for a typical case. The orbit had an altitude of 7000 km and an inclination of 0 deg and was set during solar max. This orbit is not a particularly practical orbit. It was chosen for two reasons. It resides in the middle of the Van Allan belts, where the highest concentrations of electrons are located, and geostationary satellites must fly through this region to get to geosynchronous orbit. This orbit gave a total electron flux of 2.8×10^8 #/cm^2-s with a total dose rate of 7.15 rad/s and a total proton flux of 2.9×10^7 #/cm^2-s with a total dose rate of 771 rad/s.

The material properties used for the analysis were those for a typical organic polymer (Table 1). The baseline case simulation was run with the preceding parameters, a thickness of 2.5 mm, boundary conditions of $E = V = 0$ on the back face, and without any radiation-induced conductivity. The boundary conditions were selected because they gave the highest voltages and fields. They are physically reasonable, corresponding to a conducting backplane behind the composite, grounded to a spacecraft with an overall zero net charge. The results in Fig. 3 show that it took 1.3 s to reach a steady state, with a maximum electric field of approximately 4400 V/m. This result is several orders of magnitude below the breakdown value of 15 MV/m.

The baseline case was then run with radiation-induced conductivity included. The material parameters (k_R and Δ) were selected (Table 1) to produce the most extreme case possible, i.e., the highest possible radiation-induced conductivity within the range of values for polymers. The results showed no change compared with the baseline case. The radiation-induced conductivity turned out to be small, 9.2×10^{-12} 1/Ω-m. This is approximately one order of magnitude less than the dark conductivity of the material (10^{-10} 1/Ω-m), and thus little effect was seen when the two were added together. Even though the dark conductivity of the polymer could decrease below the value of the radiation-induced conductivity, the value obtained for the radiation-induced conductivity is a worst case value, and in reality it may even be lower.

Table 1 Baseline case material properties

Property	Value
Density ρ_m	1600 kg/m^3
Thickness h	2.5 mm
Dielectric constant κ	3.0
Electrical conductivity σ	1×10^{-10} 1/Ω-m
Dielectric strength $E_{\max}$	15×10^6 V/m
Radiation-induced conductivity exponent Δ	1.0
Coefficient of radiation-induced conductivity k_R	1.1×10^{-14} s/Ω-m-rad

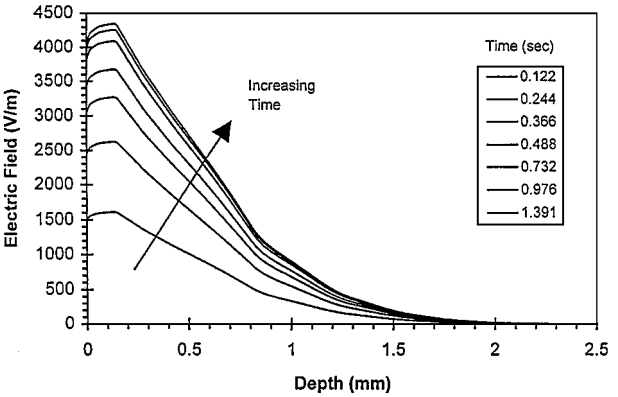

Fig. 3 Base case electric field as a function of depth.

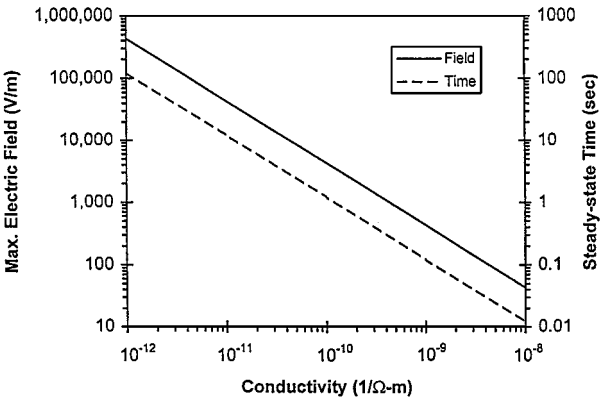

Fig. 4 Conductivity sensitivity.

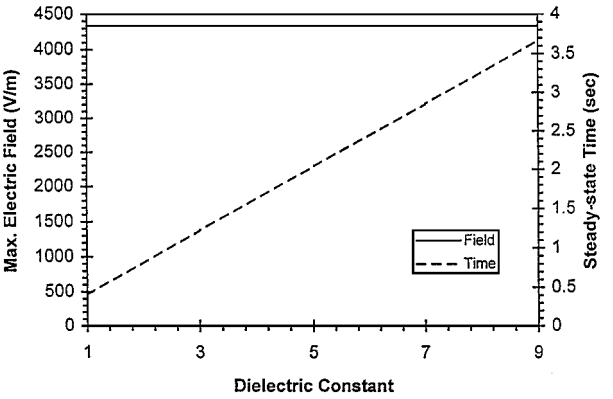

Fig. 5 Dielectric constant sensitivity.

Sensitivity studies were performed on the material properties because exact values for composites were not known. The properties that were varied were the electrical conductivity, the dielectric constant, and the input fluxes. The electrical conductivity was varied from 10^{-12} to 10^{-8} 1/Ω-m, the range of electrical conductivities for organic polymers. The results showed that an increase in conductivity produced a decrease in electric field and the time to steady state by the same order of magnitude as the conductivity increase (Fig. 4) and that there was no change in the distribution. The dielectric constant was varied from one to nine, which is the range of almost all materials. The results showed that change in the dielectric constant had no effect on the steady-state electric field but changed the time to steady state (Fig. 5). The input electron fluxes were

Table 2 Reported properties of selected materials and composites[11–14]

Material	Density, kg/m^3	Conductivity, 1/Ω-m	Dielectric constant	Dielectric strength, MV/m
Carbon fibers	1,384–2,200	2×10^4–10^6	——	0.0032–0.0044
Epoxy	1,052–2,187	10^{-8}–10^{-3}	2.78–5.2	——
Glass/epoxy	1,550–2,076	$\leq 10^{-10}$	4.2–5.68	17.7–21.7
Carbon/epoxy (longitudinal)	1,577–1,700	374–47,600	——	——
Carbon/epoxy (transverse)	——	1.5–2,000	——	——
Carbon/epoxy (through thickness)	——	0.1–106	——	——
Kapton	1,420–1,670	7×10^{-16}–10^{-15}	2.7–3.5	154–303

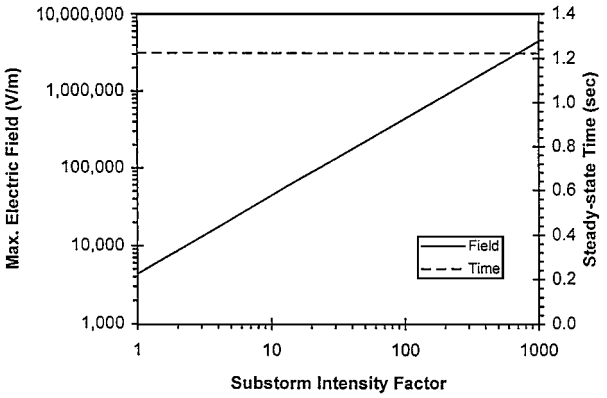

Fig. 6 Substorm sensitivity.

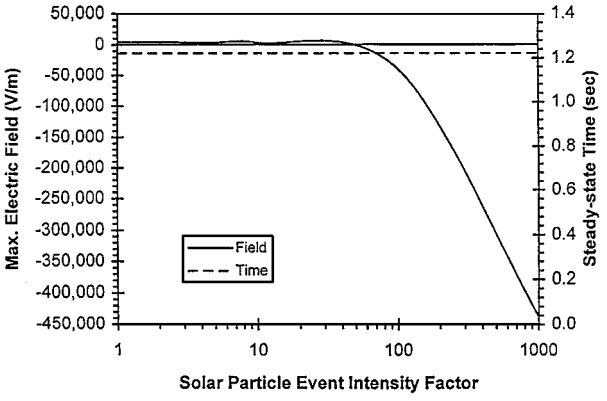

Fig. 7 Solar particle event sensitivity.

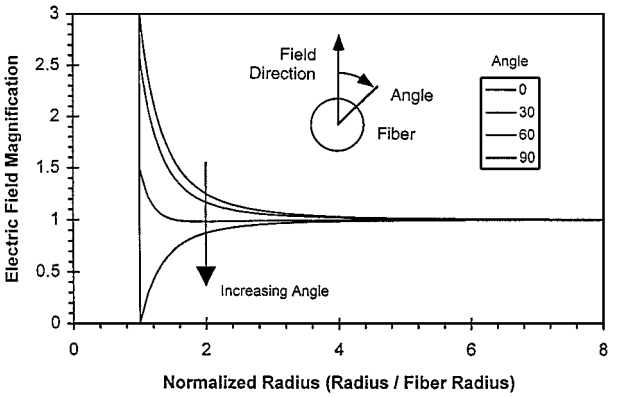

Fig. 8 Electric field magnification around a fiber.

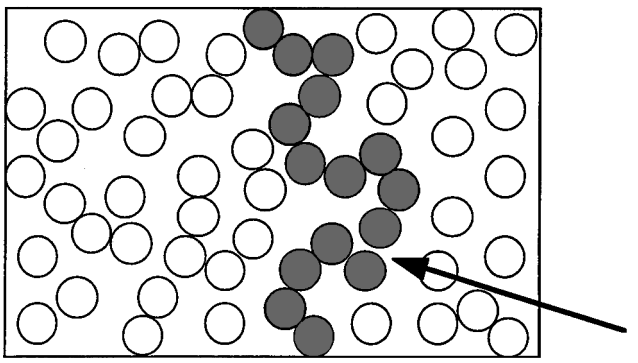

Fig. 9 Schematic of an unlikely fiber arrangement, which can lead to high electric field magnification.

increased by an intensity factor, varied from 1 to 1000, to simulate substorm data. The results showed that the maximum steady-state electric field increased linearly with the intensity factor, whereas the time to steady state remained unchanged (Fig. 6). The input proton fluxes were also increased by an intensity factor, varied from 1 to 1000, to simulate solar particle event data. The results showed that the maximum steady-state electric field remained constant until the intensity factor was large enough to start increasing the magnitude of the (negative) electric field. The time to steady state remained unchanged with increasing intensity factor (Fig. 7).

Composites

The composite material was handled on two different levels, the bulk material level and the microscale level. At the bulk level the composite material is treated as a uniform material with average material properties because the fiber diameter is much smaller than the thickness of the plies and the laminate. From Table 2[11–14] the conductivity of glass fibers is similar to that of the material assumed in the baseline case, and hence a glass-fiber composite would have similar bulk conductivity to the baseline material. The effect of somewhat lower conductivity in the glass fibers (e.g., an order of magnitude) can be seen in Fig. 4. Depending on the fiber volume fraction, packing arrangements, and micromechanical calculation methods selected, the calculated bulk composite conductivity will vary within the limits of the glass fiber conductivity (10^{-11} 1/Ω-m) and that of the polymer matrix (10^{-10} 1/Ω-m). The resulting electric field would vary by an order of magnitude or so, but stay well below the material dielectric strength. Experimental data (Table 2) show that graphite-epoxy composites have very high conductivity compared to the material of the baseline case, and hence electric field development in these materials, at least when considered in bulk, would be negligible.

At the microscale a concern is that higher fields could be possible because of the geometric details of the fibers embedded in the matrix. The micromechanics of a fiber surrounded by epoxy was examined to see if a substantial increase in the electric field can occur as the electric field in the epoxy matrix approaches the highly conductive carbon fibers. A steady-state analysis showed that the increase in the electric field is dependent on the amount of matrix between fibers and that the greatest possible increase is by a factor of three (Fig. 8). This steady-state analysis was performed by solving Eq. (1) in radial coordinates, assuming a zero-charge density and a constant electric field in the far field.

Unlikely arrangements of multiple fibers can create severe distortions in the electric fields (Fig. 9), possibly resulting in increases as high as 50 times.[15] This topic requires further study. With carbon

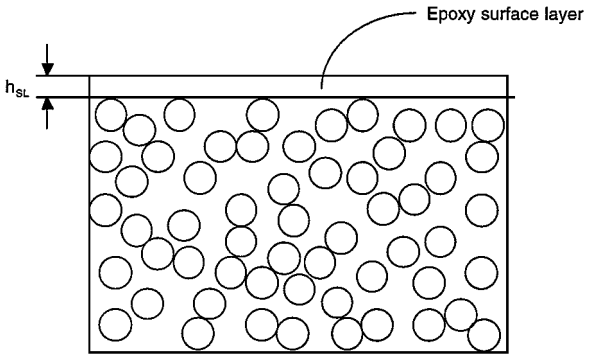

Fig. 10 Schematic of the pure epoxy surface layer.

fiber epoxy composites the electric field is very small, and even an increase of 50 times would result in a field strength insignificant compared with the material breakdown strength.

A related problem is that of the electric field in a carbon fiber epoxy composite with an epoxy-rich surface layer (Fig. 10). This layer, approximately 20 μm thick, has a much lower (by several orders of magnitude) electrical conductivity than the bulk composite. An analysis was accomplished by modifying the code to include materials with two different electrical conductivities, the bulk material conductivity and the surface layer conductivity. The results showed that the electric field in the bulk material came to a steady state as it would have in the case of only the carbon fiber epoxy composite with no epoxy layer. However, the electric field in the surface layer increased until it reached approximately the steady-state value that would be observed in the case of the composite being made of only matrix material. This situation was computationally difficult because of the small time steps required by the conductive composite combined with the slow setting time of the surface layer. A simplified model was also developed for parametric studies.[6]

Conclusions

This research has developed a tool for calculating the electric field and charge density in composite spacecraft components as functions of the depth in the material, and from this data determine whether an electrical breakdown and resulting electrostatic discharge occur. The user defines the environment by specifying the orbit parameters, the material properties, and whether radiation-induced conductivity is to be included in the analysis. These analyses do not take into account the increasing potential of the spacecraft, surface charging and discharge phenomena, or the problem of differential charging between the composite structure and neighboring components made of different materials.

Based on sensitivity studies, the conclusion was made that conductive composites, such as carbon fiber epoxy composites, are unlikely to have problems with deep dielectric charging, except possibly in nonconductive epoxy-rich surface layers. For nonconductive composites, such as glass fiber or Kevlar composites, or filled polymers, deep dielectric charging is more of a concern. Typical day-to-day flux levels do not cause concerns with deep dielectric charging, as electric fields do not reach critical values. However, electric field strengths close to or greater than the dielectric strength can arise during substorms, when particle flux levels can rise by several orders of magnitude.

This work highlights the possibility of deep dielectric charging problems in low-conductivity materials. Materials at the lower end of the possible conductivity range are at the most risk. This suggests the need for accurate material properties and a method for tailoring conductivities, so that materials can be designed with insulating properties but without extremely low values of conductivity that might create problems. These subjects are pursued in a companion paper.

References

[1]Larson, W. J., and Wertz, J. R., *Space Mission Analysis and Design*, 2nd ed., Microcosm, Torrance, CA, and Kluwer Academic, Norwell, MA, 1993, pp. 198–201.

[2]Purvis, C. K., Garrett, H. B., Whittlesey, A. C., and Stevens, N. J., "Design Guidelines for Assessing and Controlling Spacecraft Charging Effects," NASA TP-2361, Sept. 1984.

[3]Wrenn, G. L., "Conclusive Evidence for Internal Dielectric Charging Anomalies on Geosynchronous Communications Spacecraft," *Journal of Spacecraft and Rockets*, Vol. 32, No. 3, 1995, pp. 514–520.

[4]Berkley, D. A., "Computer Simulation of Charge Dynamics in Electron-Irradiated Polymer Foils," *Journal of Applied Physics*, Vol. 50, No. 5, 1979, pp. 3447–3453.

[5]Frederickson, A. R., and Woolf, S., "Electric Fields in keV Electron Irradiated Polymers," *IEEE Transactions on Nuclear Science*, Vol. NS-29, No. 6, 1982, pp. 2004–2011.

[6]Czepiela, S. A., "The Charging of Composites in the Space Environment," M.S. Thesis, Dept. of Aeronautics and Astronautics, Massachusetts Inst. of Technology, Cambridge, MA, Aug. 1997.

[7]Soubeyran, A., "Internal and Bulk Charging: Analysis of Risks and Protection Means," *Proceedings from the Space Environment: Prevention of Risks Related to Spacecraft Charging Conference*, 1996, pp. 191–205.

[8]Davis, V. A., Gardner, B. M., McGeary, C. F., Ramos, D. A., Rankin, T. V., and Wilcox, K. G., *EWB User's Reference Manual*, Ver. 3.0, S-Cubed Div. of Maxwell Lab., La Jolla, CA, 1994.

[9]Hastings, D., and Garrett, H., *Spacecraft Environment Interactions*, Cambridge Univ. Press, New York, 1996, p. 47.

[10]Griffiths, D. J., *Introduction to Electrodynamics*, 2nd ed., Prentice–Hall, Upper Saddle River, NJ, 1989.

[11]Frederickson, A. R., "Radiation Induced Currents and Conductivity in Dielectrics," *IEEE Transactions on Nuclear Science*, Vol. NS-24, No. 6, 1977, pp. 2532–2539.

[12]Kaddour, A. S., Al-Salehi, F. A. R., Al-Hassani, S. T. S., and Hinton, M. J., "Electrical Resistance Measurement Technique for Detecting Failures in CFRP Materials at High Strain Rates," *Composites Science and Technology*, Vol. 51, No. 3, 1994, pp. 377–385.

[13]Lee, S. M., *International Encyclopedia of Composites*, Vol. 3, VCH Publishers, New York, 1990, pp. 150–153.

[14]Lodge, K. J., "The Electrical Properties of Joints in Carbon Fibre Composites," *Composites*, Vol. 13, No. 3, 1982, pp. 305–310.

[15]Bent, A., "Active Fiber Composites for Structural Actuation," Ph.D. Dissertation, Dept. of Aeronautics and Astronautics, Massachusetts Inst. of Technology, Cambridge, MA, Jan. 1997.

I. D. Boyd
Associate Editor